A Bacterial Effector Acts as a Plant Transcription Factor and Induces a Cell Size Regulator

Sabine Kay *et al.*

Science **318**, 648 (2007);
DOI: 10.1126/science.1144956

genic *hrcV* mutant strain. HrcV is a conserved protein of the core T3S system with mutants incapable of delivering T3S effector proteins (*12*). After immunoprecipitation with an antibody to AvrBs3 (*13*), enrichment of the *Bs3* but not the *Bs3-E* promoter region was detected by semi-quantitative PCR (Fig. 4D). This demonstrates that *Xcv*-delivered AvrBs3 binds to the *Bs3* promoter in vivo with higher affinity than to the *Bs3-E* promoter. Given that *Bs3* promoter enrichment was detected in leaf material inoculated with the wild type but not with the *hrcV* mutant strain, we conclude that the *Bs3* promoter is bound before cell lysis.

We also infected the pepper cultivar ECW-123R containing the *R* genes *Bs1*, *Bs2*, and *Bs3* with xanthomonads delivering either the structurally unrelated AvrBs1, AvrBs2, or AvrBs3 protein or none of these Avr proteins. RT-PCR showed that the *Bs3*-derived transcripts were detectable only upon infection with *avrBs3*-expressing *Xcv* strains (fig. S10). Therefore, *Bs3* is not transcriptionally activated in the course of the *Bs1*- or *Bs2*-mediated HR.

Isolation of the pepper *Bs3* gene uncovered a mechanistically novel type of recognition mechanism and a structurally novel type of R protein that shares homology to FMOs. Recently, FMO1, an *Arabidopsis* protein that is sequence-related to Bs3 (fig. S2), was shown to be involved in pathogen defense (*14*–*16*). Thus, FMO1 and Bs3 may have similar functions. However, *FMO1* is transcriptionally induced by a variety of stimuli including virulent and avirulent microbial pathogens (*14*, *16*, *17*). In contrast, *Bs3* was not induced by virulent *Xcv* strains (Fig. 3), nor by resistance reactions mediated by the pepper *R* genes *Bs1* and *Bs2* (fig. S10). Moreover, 35S-driven *Bs3* alleles triggered an HR reaction (fig. S7), whereas a 35S-driven *FMO1* gene mediates broad-spectrum resistance but not HR (*14*, *15*). Thus, *Arabidopsis FMO1* and pepper *Bs3* differ with respect to their transcriptional regulation and function.

Our results show that the bacterial effector protein AvrBs3 binds to and activates the promoter of the matching pepper *R* gene *Bs3*. Analysis of host genes that are up-regulated by AvrBs3 ("*upa*" genes) in a compatible *Xcv*-pepper interaction (*7*, *18*) led to the identification of the *upa*-box (TATATAAACCN$_{2\text{-}3}$CC), a conserved DNA element that was shown to be bound by AvrBs3 and that is also present in the *Bs3* promoter (Fig. 1D) (*18*). This suggests that binding of AvrBs3 to the *upa*-box is crucial for activation of corresponding promoters. However, binding of an AvrBs3-like protein does not necessarily result in promoter activation, because AvrBs3Δrep16 bound with higher affinity to the *Bs3* than to the *Bs3-E* promoter (fig. S9) but only activated the *Bs3-E* and not the *Bs3* promoter (Fig. 3). Because AvrBs3Δrep16 and AvrBs3 differ in their structure, we postulate that upon DNA binding, their functional domains (e.g., AD) are exposed at different promoter locations, which may define whether AvrBs3Δrep16 and AvrBs3 are able to activate a given promoter. Additionally, given that the *Bs3* promoter determines recognition specificity, the *Bs3* promoter might be coevolving to maintain compatibility with rapidly changing AvrBs3-like proteins, similar to that seen in the NB-LRR proteins (*19*, *20*).

We consider it likely that not only AvrBs3 but also other AvrBs3 homologs bind to and activate promoters of matching *R* genes. The recently isolated rice *R* gene *Xa27*, which mediates recognition of the AvrBs3-like AvrXa27 protein from *Xanthomonas oryzae* pv. *oryzae* (*21*), is transcriptionally induced by AvrXa27, and thus it is tempting to speculate that the *Xa27* promoter is a direct target of AvrXa27. However, whether AvrXa27 acts directly at the *Xa27* promoter remains to be clarified.

References and Notes

1. J. D. Jones, J. L. Dangl, *Nature* **444**, 323 (2006).
2. F. Thieme *et al.*, *J. Bacteriol.* **187**, 7254 (2005).
3. S. Schornack, A. Meyer, P. Römer, T. Jordan, T. Lahaye, *J. Plant Physiol.* **163**, 256 (2006).
4. K. Herbers, J. Conrads-Strauch, U. Bonas, *Nature* **356**, 172 (1992).
5. B. Szurek, E. Marois, U. Bonas, G. Van den Ackerveken, *Plant J.* **26**, 523 (2001).
6. B. Szurek, O. Rossier, G. Hause, U. Bonas, *Mol. Microbiol.* **46**, 13 (2002).
7. E. Marois, G. Van den Ackerveken, U. Bonas, *Mol. Plant Microbe Interact.* **15**, 637 (2002).
8. G. Van den Ackerveken, E. Marois, U. Bonas, *Cell* **87**, 1307 (1996).
9. T. Jordan *et al.*, *Theor. Appl. Genet.* **113**, 895 (2006).
10. U. Bonas, J. Conrads-Strauch, I. Balbo, *Mol. Gen. Genet.* **238**, 261 (1993).
11. N. L. Schlaich, *Trends Plant Sci.* **12**, 412 (2007).
12. O. Rossier, K. Wengelnik, K. Hahn, U. Bonas, *Proc. Natl. Acad. Sci. U.S.A.* **96**, 9368 (1999).
13. V. Knoop, B. Staskawicz, U. Bonas, *J. Bacteriol.* **173**, 7142 (1991).
14. M. Bartsch *et al.*, *Plant Cell* **18**, 1038 (2006).
15. M. Koch *et al.*, *Plant J.* **47**, 629 (2006).
16. T. E. Mishina, J. Zeier, *Plant Physiol.* **141**, 1666 (2006).
17. B. Olszak *et al.*, *Plant Sci.* **170**, 614 (2006).
18. S. Kay, S. Hahn, E. Marois, G. Hause, U. Bonas, *Science* **318**, 648 (2007).
19. J. M. McDowell, S. A. Simon, *Mol. Plant Pathol.* **7**, 437 (2006).
20. J. G. Ellis, P. N. Dodds, G. J. Lawrence, *Annu. Rev. Phytopathol.* **45**, 289 (2007).
21. K. Gu *et al.*, *Nature* **435**, 1122 (2005).

22. We thank N. Collins, L. Rose, J. Parker, M. Dow, C. Peterhänsel, E. Marois, N. Schlaich, C. Pabst, S. Schornack, A. Strauß, and S. Kay for helpful comments and suggestions on the manuscript, and H. Scholze, B. Rosinsky, and C. Kretschmer for excellent technical assistance. T. Nakagawa provided the pGWB vector series. Supported by funds from the Deutsche Forschungsgemeinschaft to T.L. (LA 1338/2-2) and U.B. (SFB 648). *Bs3* and *Bs3-E* sequences have been deposited in GenBank with accession numbers EU078684 and EU078683, respectively.

Supporting Online Material

www.sciencemag.org/cgi/content/full/318/5850/645/DC1
Materials and Methods
Figs. S1 to S10
References

10 May 2007; accepted 21 September 2007
10.1126/science.1144958

A Bacterial Effector Acts as a Plant Transcription Factor and Induces a Cell Size Regulator

Sabine Kay,[1] Simone Hahn,[1] Eric Marois,[1]* Gerd Hause,[2] Ulla Bonas[1]†

Pathogenicity of many Gram-negative bacteria relies on the injection of effector proteins by type III secretion into eukaryotic cells, where they modulate host signaling pathways to the pathogen's benefit. One such effector protein injected by *Xanthomonas* into plants is AvrBs3, which localizes to the plant cell nucleus and causes hypertrophy of plant mesophyll cells. We show that AvrBs3 induces the expression of a master regulator of cell size, *upa20*, which encodes a transcription factor containing a basic helix-loop-helix domain. AvrBs3 binds to a conserved element in the *upa20* promoter via its central repeat region and induces gene expression through its activation domain. Thus, AvrBs3 and likely other members of this family provoke developmental reprogramming of host cells by mimicking eukaryotic transcription factors.

Gram-negative phytopathogenic bacteria of the genus *Xanthomonas* cause a broad variety of diseases in crop plants (*1*). Pathogenicity depends on the translocation of effector proteins directly into the plant cell cytosol by a type III secretion (T3S) system (*2*). The AvrBs3 family is a prominent effector class in *Xanthomonas* spp. (*3*), comprising major virulence determinants (*4*–*6*). These effectors are characterized by a central repeat region, nuclear localization signals (NLSs), and an acidic transcriptional activation domain (AD) (*3*). AvrBs3 was isolated from *X. campestris* pv. *vesicatoria* (*Xcv*), the causal agent of bacterial spot disease on pepper and tomato (*7*). In susceptible host plants and other solanaceous species, AvrBs3 elicits hypertrophy (i.e., enlargement) of mesophyll cells (*8*) and also contributes to the dispersal of *Xcv* between pepper plants under field conditions (*9*). Cell enlargement is also found in other complex disease phenotypes [e.g., citrus canker elicited by the AvrBs3-like effector PthA from *X. axonopodis* pv. *citri* (*10*) and *Pantoea agglomerans*–induced gall formation (*11*)].

AvrBs3 has a central region consisting of 17.5 nearly identical 34–amino acid repeats [which determine the specificity of protein activity in plants (*8*, *12*)], functional NLSs, and an AD in its C terminus (*13*–*15*)—all of which are essential for AvrBs3 activity. Furthermore, AvrBs3 forms homodimers (*16*) and appears to be a transcription factor localized to the plant cell nucleus (*8*, *13*–*15*). Pepper *upa* (upregulated by AvrBs3) genes that are induced by AvrBs3 encode, amongst others, putative α-expansins and auxin-induced proteins that might be involved in the induction of hypertrophy (*8*). However, most *upa* genes are indirect targets of AvrBs3 because their induction requires de novo synthesis of plant proteins (*8*).

To isolate *upa* genes that are direct targets of AvrBs3, we infected susceptible pepper plants [cultivar Early Calwonder (ECW)] with *Xcv* strain 85-10 expressing *avrBs3* or carrying an empty vector in the presence of cycloheximide, which blocks eukaryotic protein synthesis. cDNA fragments corresponding to AvrBs3-induced pepper genes were identified by suppression-subtractive hybridization and confirmed by reverse Northern analysis and reverse transcription polymerase chain reaction (RT-PCR). Among these cDNAs, we detected the previously identified *upa10* and *upa11* genes (*8*), validating our approach, as well as previously unrecognized AvrBs3-induced genes. One gene, designated *upa20*, encodes a putative transcription factor of the basic helix-loop-helix (bHLH) family and was chosen for further analysis.

We isolated the full-length cDNA of *upa20* by rapid amplification of cDNA ends (RACE)–PCR and determined the corresponding genomic sequence from a pepper BAC (bacterial artificial chromosome) library (*17*). *upa20* has a complex gene structure comprising eight exons and seven introns (Fig. 1A) and encodes a putative 340–amino acid bHLH transcription factor with a predicted molecular mass of 37.8 kD. The bHLH domain, which generally serves as DNA binding and dimerization domain (*18*), is located in the region from amino acids 167 to 225 (Fig. 1B). BLASTP analyses show that Upa20 is most related to an uncharacterized protein from rice (Os09g0510500; accession BAF25548.1; 48% identity and 63% similarity over 240 amino acids) and is also similar to BIGPETALp (BPEp) from *Arabidopsis* (accession CAK32499.1; 55% identity and 70% similarity over 134 amino acids), which is involved in the control of petal size (*19*).

To address the role of *upa20* in the induction of hypertrophy, we performed virus-induced gene silencing of *upa20* in *Nicotiana benthamiana*, which severely reduced the normally strong AvrBs3-dependent hypertrophy, the result of which was visible as pustules on the lower leaf surface (Fig. 2, A and B). *Agrobacterium*-mediated *upa20* expression demonstrated that Upa20 alone induces hypertrophy in *N. benthamiana* and other solanaceous plants (Fig. 2C and fig. S1). In *upa20*-expressing tissue of *N. benthamiana*, palisade and spongy parenchyma cells were strongly enlarged as compared with those in tissue of the control (Fig. 2, D and F). The hypertrophy reaction was phenotypically similar to tissue transiently expressing *avrBs3* (Fig. 2E) but was faster and stronger. Further observations revealed cell wall invaginations exclusively in *upa20*-expressing tissue, suggesting that cell wall synthesis is increased (Fig. 2, G and H). In addition, chloroplasts of *upa20*-expressing cells showed a decrease in starch content (Fig. 2, I and J) in accordance with cell enlargement being a highly energy-consuming process. Therefore, our re-

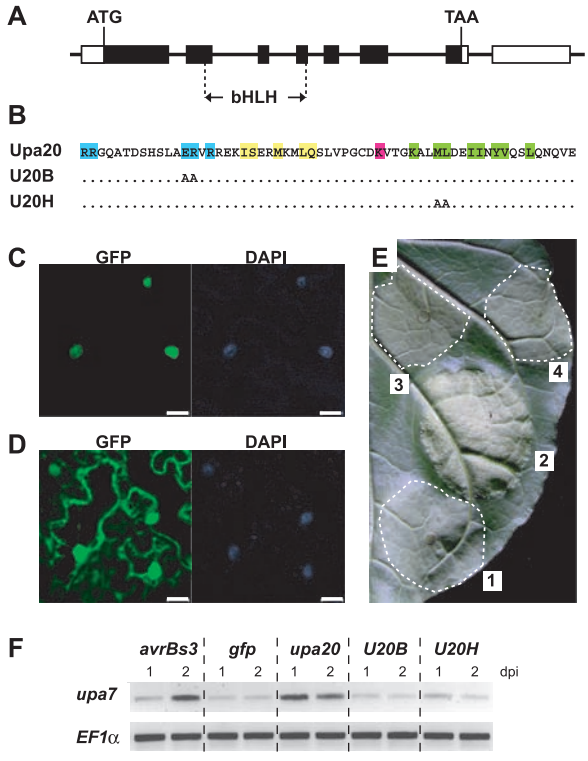

Fig. 1. (**A**) Structure of *upa20* in pepper. Coding and noncoding exons are indicated as black and white rectangles, and introns are indicated as black lines between the exons. (**B**) Amino acid sequence (*30*) of the Upa20 bHLH region (amino acids 167 to 225). The amino acids that define the bHLH motif (*18*) are color-coded (basic region, blue; first helix, yellow; loop, pink; and second helix, green). Conserved amino acids were changed to alanine in the basic region (U20B) and in the HLH dimerization motif (U20H). (**C** and **D**) Confocal laser scanning microscopy of *N. benthamiana* 2 days after *Agrobacterium*-mediated transfer of *upa20::gfp* (C) or *gfp* (D). 4′,6′-Diamidino-2-phenylindole (DAPI) staining indicates nuclei. Scale bars, 20 μm. (**E**) *N. benthamiana* transiently expressing *gfp* (1), *upa20::c-myc* (2), *U20B::c-myc* (3), and *U20H::c-myc* (4), 8 days post-infiltration (dpi). (**F**) Upa20 induces the expression of *upa7*, encoding a putative α-expansin. RT-PCR analysis of susceptible pepper plants 1 and 2 dpi of *Agrobacterium* delivering *avrBs3*, *gfp*, *upa20*, *U20B*, and *U20H*, respectively, is shown. *EF1*α was used as control for equal cDNA amounts.

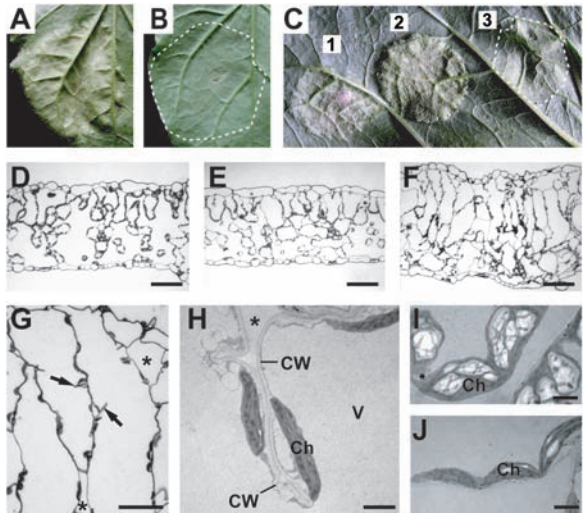

Fig. 2. (**A** and **B**) Transient expression of *avrBs3* elicits a hypertrophy in *gfp*-silenced (A), but not in *upa20*-silenced (B), *N. benthamiana* leaves, 11 dpi. (**C**) *Agrobacterium*-mediated expression of *avrBs3* (1) and *upa20* (2) causes hypertrophy in *N. benthamiana* 7 dpi relative to control [empty transferred DNA (T-DNA) (3)]. (**D** to **F**) Light microscopy of *N. benthamiana* leaves 4 days after *Agrobacterium*-mediated delivery of empty T-DNA (D), *avrBs3* (E), and *upa20* (F). (**G**) Higher magnification of a sector in (F). Arrows indicate cell wall invaginations. (**H**) Electron micrograph of a cell wall invagination of an *N. benthamiana* palisade cell expressing *upa20*, 4 dpi. Asterisks in (G) and (H) mark apoplastic spaces. (**I** and **J**) Chloroplasts of *N. benthamiana* cells 3 dpi with *Agrobacterium* delivering an empty T-DNA (I) or *upa20* (J). Scale bars correspond to 100 μm [(D) to (F)], 30 μm (G), and 2 μm [(H) to (J)], respectively. Ch, chloroplast; CW, cell wall; V, vacuole.

[1]Institute of Biology, Department of Genetics, Martin-Luther-University Halle-Wittenberg, Weinbergweg 10, D-06120 Halle (Saale), Germany. [2]Biozentrum, Martin-Luther-University Halle-Wittenberg, Weinbergweg 22, D-06120 Halle (Saale), Germany.

*Present address: Institut de Biologie Moléculaire et Cellulaire, CNRS Unité Propre de Recherche 9022, 15 rue René Descartes, F-67084 Strasbourg, France.

†To whom correspondence should be addressed. E-mail: ulla.bonas@genetik.uni-halle.de

sults suggest that Upa20 is a master regulator of cell enlargement that stimulates cell growth, in contrast to BPEp from *Arabidopsis*, which reduces cell size (*19*). Consistent with its predicted function as a transcription factor, N- and C-terminal green fluorescent protein (GFP) fusions of Upa20 were exclusively localized to the nucleus, where they often concentrated in distinct foci (Fig. 1C and fig. S2). These foci are reminiscent of nuclear speckles, which may be storage and assembly areas of transcription and splicing factors, supplying them to active transcription sites (*20*). When the basic region (U20B) and the dimerization domain (U20H) of Upa20 were altered (Fig. 1B), both mutants failed to cause hypertrophy in *N. benthamiana* (Fig. 1E), although all proteins were expressed in similar amounts (fig. S3).

Together, these results suggest that Upa20 is a bona fide bHLH transcription factor. We wondered whether any of the previously identified *upa* genes are target genes of Upa20. Induction of *upa1* to *upa9*, expression of which requires de novo protein synthesis, starts 6 to 9 hours after infection of pepper plants with *Xcv* delivering AvrBs3 (*8*), whereas *upa20* induction starts within 3 to 4 hours post-infection (hpi) (fig. S4). RT-PCR was performed with RNA from susceptible pepper plants transiently expressing *upa20* and the *upa20* bHLH mutants along with controls. Upa20 activated the expression of *upa7*, encoding a putative α-expansin, which was shown to be dependent on the bHLH domain of Upa20 (Fig. 1F). However, the other genes tested were not consistently induced by Upa20, suggesting that AvrBs3 activates additional genetic pathways.

Our results indicate that the visible consequence of AvrBs3 virulence activity in susceptible plants, the induction of cell hypertrophy, is caused by AvrBs3 targeting *upa20*, a regulator of cell enlargement. To elucidate the mechanism of *upa20* induction, we tested for the requirement of the eukaryotic motifs in AvrBs3. Pepper plants infected with *Xcv* expressing *avrBs3* and mutant derivatives clearly showed that both the NLSs and AD are required for gene activation (fig. S5). In addition, deletion of four repeats abolished *upa20* induction (fig. S5), demonstrating that the central repeat region of AvrBs3 is indispensable for function. Similarly, the AvrBs3 homolog AvrBs4, which differs from AvrBs3

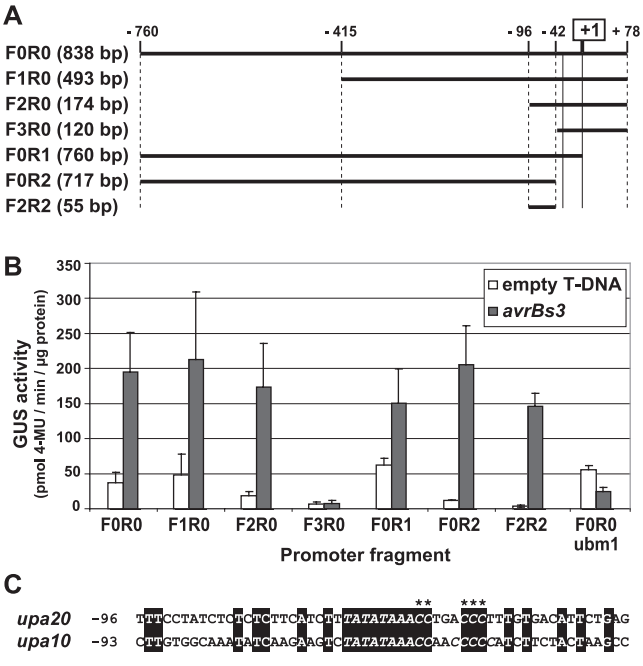

Fig. 3. (**A**) Promoter fragments tested for AvrBs3 inducibility. The transcriptional start sites, in the presence of AvrBs3 (+1) and predominantly used in the absence of AvrBs3 (37 bp upstream of +1), are indicated with solid vertical lines. The transcription start of F0R2 was mapped to the *att*B2 site of the construct. Dashed lines and numbers above indicate positions with respect to +1. (**B**) GUS assays show AvrBs3 inducibility of the *upa20* promoter in *N. benthamiana*. Promoter fragments shown in (A) and a *upa* box mutant derivative of F0R0, F0R0ubm1 [see (C)], were cloned in front of a *egfp::uidA* reporter and tested by codelivery with *avrBs3* and empty T-DNA. 4-MU, 4-methylumbelliferone. Error bars indicate SD. (**C**) The smallest AvrBs3-responsive *upa20* promoter fragment (F2R2) (top row) as compared with a corresponding region in the *upa10* promoter. Numbers refer to the transcriptional start site (+1) in the presence of AvrBs3. Nucleotides that belong to the proposed *upa* box are indicated in italics. Asterisks mark nucleotides that were changed to G in mutant ubm1.

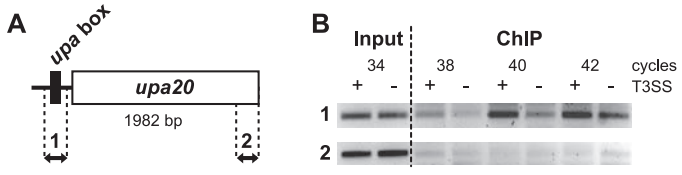

Fig. 4. (**A**) Fragments in the pepper *upa20* region analyzed by ChIP. (**B**) ChIP analysis of pepper ECW 12 hpi with *Xcv* strain 82-2 (+T3SS) and the T3S system mutant 82-8Δ*hrcV* (–T3SS). Fragments surrounding [(1); 197 bp] and downstream of the *upa* box [(2); 209 bp] [see (A)] were amplified with cycle numbers as indicated. (**C**) EMSA with increasing molar amounts of GST::AvrBs3 incubated with 50 fmol biotin-labeled 36-bp *upa20* promoter fragments containing the *upa* box. The control is GST. Unlabeled WT fragments and fragments with a mutated *upa* box (ubm1, see Fig. 3C) were used as competitor DNA. (**D**) EMSA of 50 fmol biotin-labeled WT promoter fragment incubated with increasing amounts of GST::AvrBs3ΔN+C (AvrBs3 repeat region) and GST::AvrBs3Δrepeats. Unlabeled WT DNA fragments were used for competition. Arrows, bound probe; asterisks, free probe. The uppermost signals correspond to DNA in the slots. For expression of the GST fusion proteins, see fig. S9.

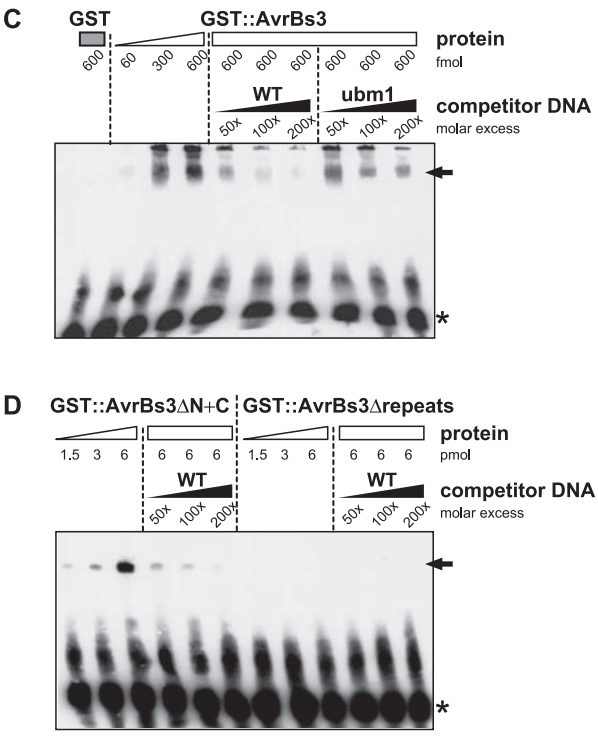

mainly in the repeat region (*21*), does not enhance *upa20* expression, which is in agreement with the finding that AvrBs3 deletion derivatives and AvrBs4 do not induce a hypertrophy (*8*).

To identify an AvrBs3-responsive DNA element, we isolated the promoter and determined the transcription start site of *upa20*. Comparison of cDNA sequences revealed that, in the presence of AvrBs3, transcription of *upa20* starts 37 base pairs (bp) downstream of the prevalent start site used for the basal level of *upa20* transcription under non-inducing conditions (fig. S6). Upstream of both transcription start sites, a TATA box motif is located (fig. S6). These data suggest that *upa20* undergoes alternative transcriptional initiation, which has been reported for a wide range of eukaryotic genes (*22*, *23*) and is probably mediated by the action of different transcription factors.

To analyze the AvrBs3 inducibility of the *upa20* promoter, we used a promoterless *egfp::uidA* cassette as a reporter in *N. benthamiana* after *Agrobacterium*-mediated transformation. β-Glucuronidase (GUS) activities and GFP fluorescence revealed that the *upa20* promoter is AvrBs3-responsive (Fig. 3B and fig. S7). Promoter deletions from both ends limited the AvrBs3-responsive region to a 55-bp sequence (Fig. 3, A and B). We searched for sequence similarities in the promoters of other putative direct targets of AvrBs3, concentrating on *upa10* (*8*). The *upa10* promoter was isolated from pepper ECW by genome walking and revealed a motif in common with the *upa20* promoter that we termed the *upa* box (Fig. 3C). This motif contains a TATA box followed by two stretches of cytosine residues, separated by two and three other nucleotides, respectively. We exchanged all cytosines (Cs) of the motif with guanines (Gs) (asterisks in Fig. 3C; this mutant was designated ubm1), which abolished the induction of the reporter gene by AvrBs3 without affecting the basal activity of the *upa20* promoter. Notably, the *upa* box is also present in the promoter of the *Bs3* resistance gene, whose activation by AvrBs3 leads to the induction of cell death in the resistant pepper line ECW-30R (*24*). In susceptible ECW plants, a 13-bp insertion between the two C stretches in the *upa* box also abolishes gene induction (*24*).

We performed chromatin immunoprecipitation (ChIP) with an AvrBs3-specific antibody (*25*) to determine whether AvrBs3 associates with the *upa20* promoter in planta. Chromatin was isolated from pepper ECW infiltrated with *Xcv* strain 82-8 naturally expressing *avrBs3* and a T3S mutant derivative (82-8Δ*hrcV*) that expresses *avrBs3* but is not able to translocate effector proteins into the plant cell (*26*). AvrBs3 precipitated with the *upa20* promoter containing the *upa* box but not with a sequence located 2 kb downstream of the *upa* box (Fig. 4, A and B). This demonstrates that DNA binding is specific, albeit it is not clear whether AvrBs3 binding is mediated by a plant protein.

Although AvrBs3 does not contain a classical DNA binding domain (*3*), we tested whether it directly interacts with the *upa20* promoter DNA in electrophoretic mobility shift assays (EMSAs) with a 36-bp biotin-labeled *upa20* promoter fragment containing the *upa* box. Addition of GST::AvrBs3 identified a protein-DNA complex with levels that increased as increasing amounts of fusion protein were added, whereas glutathione *S*-transferase (GST) alone failed to bind DNA (Fig. 4C). The band shift was competed when unlabeled *upa* box DNA was added, whereas the ubm1 fragment (Fig. 3C) competed in binding to a much lesser extent (Fig. 4C), demonstrating that AvrBs3 is specifically binding to the *upa* box. In addition, EMSA with a biotin-labeled ubm1 fragment confirmed a weaker binding of AvrBs3 to the mutant as compared with that to the wild-type (WT) sequence (fig. S8A), and this binding was competed more efficiently by the unlabeled WT sequence than by the unlabeled ubm1 fragment (fig. S8B).

An AvrBs3 derivative consisting of only the repeat region bound the *upa20* promoter fragment in EMSA, albeit less efficiently than the WT protein. In contrast, a protein containing the N and C termini of AvrBs3 but lacking the repeats did not bind (Fig. 4D). These data suggest that the 17.5 repeats in the central region of AvrBs3 mediate the specific interaction with DNA, which is consistent with the fact that the repeat region determines the specificity of AvrBs3 activity (*8*, *12*), including *upa20* induction (fig. S5). The AvrBs3 family member AvrXa7 shows an in vitro DNA binding activity with a preference for adenine-thymine (AT)–rich DNA (*27*). Our finding (that C-to-G mutations without change in AT content affected both binding of AvrBs3 in vitro and activation of the *upa20* promoter in planta) demonstrates that specificity, not base composition, determines binding.

Previously, induction of host genes has been reported for the AvrBs3-like effectors PthXo1 and AvrXa27 from the rice pathogen *X. oryzae* pv. *oryzae*. Both proteins differentially induce rice genes on the basis of their promoter variations (*28*, *29*). Sequence polymorphisms are located within 80 bp upstream of the transcription start sites (*28*, *29*) (i.e., in a similar position relative to the *upa* box in AvrBs3-responsive promoters). However, the *upa* box is not found in the rice gene promoters, suggesting that AvrBs3-like proteins have different DNA binding specificities, which are mediated by the corresponding repeat regions. The nearly identical repeats of AvrBs3-like effectors usually differ at amino acid positions 12 and 13 (*3*); hence, these amino acids might be involved in the specific interaction with DNA. How the highly similar effector proteins confer different DNA binding specificities is enigmatic and awaits the structural analysis of AvrBs3 and its homologs. In light of our data, we propose that the molecular principle of AvrBs3 action may be common to other members of this large and important family of type III effectors in bacterial plant pathogens.

References and Notes

1. F. Leyns, M. De Cleene, J. G. Swings, J. De Ley, *Bot. Rev.* **50**, 308 (1984).
2. A. P. Tampakaki, V. E. Fadouloglou, A. D. Gazi, N. J. Panopoulos, M. Kokkinidis, *Cell. Microbiol.* **6**, 805 (2004).
3. D. Gürlebeck, F. Thieme, U. Bonas, *J. Plant Physiol.* **163**, 233 (2006).
4. Y. Yang, Q. Yuan, D. W. Gabriel, *Mol. Plant-Microbe Interact.* **9**, 105 (1996).
5. B. Yang, F. F. White, *Mol. Plant-Microbe Interact.* **17**, 1192 (2004).
6. J. Bai, S.-H. Choi, G. Ponciano, H. Leung, J. E. Leach, *Mol. Plant-Microbe Interact.* **13**, 1322 (2000).
7. U. Bonas, R. E. Stall, B. J. Staskawicz, *Mol. Gen. Genet.* **218**, 127 (1989).
8. E. Marois, G. Van den Ackerveken, U. Bonas, *Mol. Plant-Microbe Interact.* **15**, 637 (2002).
9. G. Wichmann, J. Bergelson, *Genetics* **166**, 693 (2004).
10. Y. P. Duan, A. Castaneda, G. Zhao, G. Erdos, D. W. Gabriel, *Mol. Plant-Microbe Interact.* **12**, 556 (1999).
11. L. Chalupowicz, I. Barash, M. Schwartz, R. Aloni, S. Manulis, *Planta* **224**, 429 (2006).
12. K. Herbers, J. Conrads-Strauch, U. Bonas, *Nature* **356**, 172 (1992).
13. G. Van den Ackerveken, E. Marois, U. Bonas, *Cell* **87**, 1307 (1996).
14. B. Szurek, E. Marois, U. Bonas, G. Van den Ackerveken, *Plant J.* **26**, 523 (2001).
15. B. Szurek, O. Rossier, G. Hause, U. Bonas, *Mol. Microbiol.* **46**, 13 (2002).
16. D. Gürlebeck, B. Szurek, U. Bonas, *Plant J.* **42**, 175 (2005).
17. T. Jordan *et al.*, *Theor. Appl. Genet.* **113**, 895 (2006).
18. G. Toledo-Ortiz, E. Huq, P. H. Quail, *Plant Cell* **15**, 1749 (2003).
19. J. Szécsi *et al.*, *EMBO J.* **25**, 3912 (2006).
20. A. I. Lamond, D. L. Spector, *Nat. Rev. Mol. Cell Biol.* **4**, 605 (2003).
21. U. Bonas, J. Conrads-Strauch, I. Balbo, *Mol. Gen. Genet.* **238**, 261 (1993).
22. Y. Suzuki *et al.*, *EMBO Rep.* **2**, 388 (2001).
23. N. Kitagawa *et al.*, *Bioinformatics* **21**, 1758 (2005).
24. P. Römer *et al.*, *Science* **318**, 645 (2007).
25. V. Knoop, B. Staskawicz, U. Bonas, *J. Bacteriol.* **173**, 7142 (1991).
26. O. Rossier, K. Wengelnik, K. Hahn, U. Bonas, *Proc. Natl. Acad. Sci. U.S.A.* **96**, 9368 (1999).
27. B. Yang, W. Zhu, L. B. Johnson, F. F. White, *Proc. Natl. Acad. Sci. U.S.A.* **97**, 9807 (2000).
28. K. Gu *et al.*, *Nature* **435**, 1122 (2005).
29. B. Yang, A. Sugio, F. F. White, *Proc. Natl. Acad. Sci. U.S.A.* **103**, 10503 (2006).
30. Single-letter abbreviations for the amino acid residues are as follows: A, Ala; C, Cys; D, Asp; E, Glu; F, Phe; G, Gly; H, His; I, Ile; K, Lys; L, Leu; M, Met; N, Asn; P, Pro; Q, Gln; R, Arg; S, Ser; T, Thr; V, Val; W, Trp; and Y, Tyr.

31. We thank C. Gatz, R. Kahmann, F. Thieme, J. Boch, and T. Lahaye for critical reading of the manuscript, B. Rosinsky, C. Kretschmer, and S. Jahn for technical assistance, and T. Nakagawa for providing pGWB vectors. This work was funded by grants from the Deutsche Forschungsgemeinschaft to U.B. and G.H. (SFB 648 "Molekulare Mechanismen der Informationsverarbeitung in Pflanzen"). The *upa20* cDNA and genomic sequences are accession numbers EU046275 and EU046276 in GenBank.

Supporting Online Material

www.sciencemag.org/cgi/content/full/318/5850/648/DC1
Materials and Methods
Figs. S1 to S9
Table S1
References and Notes

10 May 2007; accepted 5 September 2007
10.1126/science.1144956